TENTH AUSTRALASIAN FLUID MECHANICS
CONFERENCE - UNIVERSITY OF MELBOURNE
11-15 DECEMBER 1989

THE USE OF IMAGE PROCESSING IN TURBULENT MIXING AND COMBUSTION EXPERIMENTS

T.C. CHEW and R.E. BRITTER

Department of Engineering
University of Cambridge, Trumpington St., Cambridge CB2 1PZ
ENGLAND

Abstract

We describe our experience in applying quantitative image processing techniques to flow visualisation experiments. These include studies in turbulent combustion and turbulent mixing. It is found that, while general image processing techniques such as spatial filtration, threshold discrimination and false colour representation proved essential and useful, many requirements necessitated the development of specific algorithms. Such requirements arise from both the nature of the images recorded as well as the kind of information sought. For example, to obtain the spatial correlations of burnt/unburnt states in laser tomography of premixed flames, the intensity at operator-defined grid points are recorded for a temporally deforming flame captured on video, a process termed multi-point Mie scattering. Non-standard algorithms are also needed to derive certain geometrical parameters such as flamelet crossing lengths and orientations. The evaluation of the fractal dimension of wrinkled lines requires the extraction of boundaries as a set of ordered points, or alternatively, the recursive use of spatial low-pass filters. In studying concentration fields in mixing experiments, the effect of varying the measurement volume size on concentration fluctuations can again be studied by spatial averaging. Sample results are presented for the above situations.

Introduction

The advent of laser sheet and other optical techniques in fluid flow studies has opened up new possibilities for quantitative measurements to be made from flow visualisation experiments. Increasingly such data are being sought for the development of advanced models as well as for better physical understanding.

We report here some of our experience in setting up a PC-based image processing system for post processing results from laser sheet flow visualisation experiments in reacting and non-reacting turbulent flows.

The basic system used is an IBM PC-AT microcomputer fitted with a frame grabber of 512x512x8 bit resolution, and optionally, also a 16-bit frame processing to speed up convolutions or a high speed array processor to reduce the time required for Fourier transforms. Variants of such a system are widely available on the market, with slight differences in speed and storage memory size. The major determinant of performance lies in the quality of the application software.

Popular software packages usually comprise a menu-driven environment in which a large range of image processing operations can be implemented. These will include false colour representation, frame grabber, storage and recall, filters, window operations, frame addition and subtraction, etc. More sophisticated packages allow a 'learn' option with which the user can link a series of steps into a macro.

The major drawback in most commercially available software is the inability to integrate with user-written modules. Since the aims in processing of pictures obtained from flow visualisation in fluid mechanics is fundamentally different from traditional vision and pattern recognition applications, there are numerous instances in which it is essential to create new functions and algorithms. Fortunately, most frame grabber boards are usually also supplied with a library of subroutines which perform elementary functions, for example reading and assigning the value of a pixel. These become the most useful basic building blocks.

We shall present some examples of specific applications encountered, which we believe to be in fact quite general in fluid flow studies.

Application to laser tomography of flames

Experimentally, instantaneous cross-sections of turbulent premixed flames are captured on to film and video, Chew *et al* (1989a). The flame surfaces, which appear as the interfaces separating the dark and bright regions, are thin and highly wrinkled; an example is shown in Figure 1a below. Currently, much modelling relies on a good decription and understanding of the structure of such flames.

In one formulation of the model for turbulent premixed combustion by Bray, Moss and Libby (the so-called BML model, e.g. Bray *et al* 1984) the rate of reaction is expressed in terms of geometrical parameters that can be deduced from images such as Figure 1. This includes the mean reaction progress variable $\bar{c}$, the contours where $\bar{c}$ = a constant, the number of intersections between the instantaneous (highly wrinkled) flame and the (smooth) $\bar{c}$ contour, and the orientation of the flame elements in space (see Chew *et al* 1989b).

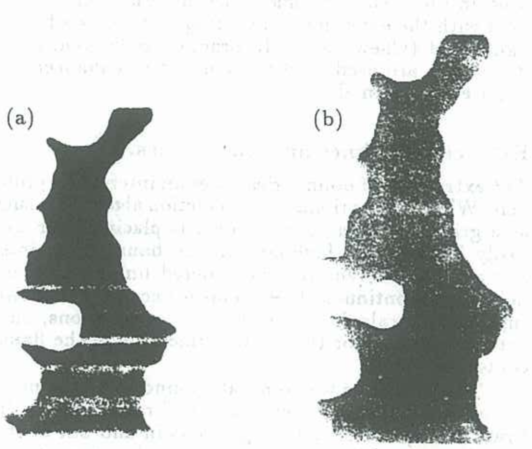

Figure 1 (a) Photograph of an instantaneous cross-section of a Bunsen flame (b) Reduced to bi-polar image.

Video images

The framing rate (25 frames per second) of normal CCD video cameras is insufficient to resolve the temporal development of the turbulent flame. However, with a gating time of $1ms$, it is possible to freeze the motion of the flame for conditions of weak turbulence. A simple procedure, termed multi-point Mie scattering, can then be used to perform interesting analysis on the video sequence. An array of grid points is first defined over the flame zone. The pixel intensity for each point is recorded for each frame as the tape is run through. Subsequently, the reacted state (burnt or unburnt) for each point is identified (by setting a simple threshold criterion on the pixel intensity). The spatial cross-correlation of the reacted states at all the points may be found. As an example, Figure 2 shows the correlation between the point X and all the other points in an 11 × 11 grid. The correlation coefficient can be integrated over the grid to find the characteristic length scales of the flame in any direction. Data to date suggest that there is a strong relationship between the integral length scale of flame wrinkling and the length scales of the turbulence in the approach flow (Chew *et al* 1989b).

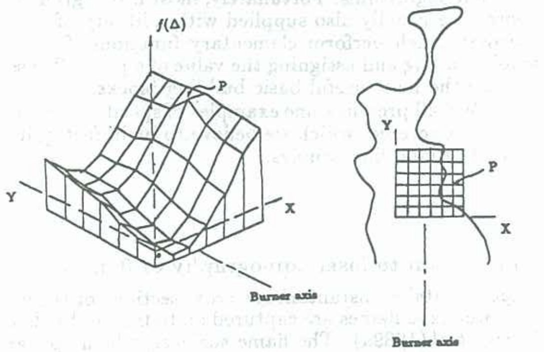

Figure 2 Cross-correlation of reaction rate over a 11×11 grid.

Images recorded on film.

After digitisation, the quality of the images which were recorded on 35mm film can be enhanced by standard image processing techniques. If necessary, single pixel noise is removed by median filtration, while suitably selected threshold discriminators are used to obtain a bi-polar picture, where the boundary separating the bright and dark regions corresponds to the flame front (Fig 1b). Sometimes special threshold operators are used in order to overcome some imperfections associated with the experimental technique, such as a fading light sheet (Chew 1988). In practice, only good quality images are used, and the amount of enhancement required is minimal.

Extraction of lines and boundaries.

The extraction of boundaries poses an interesting problem. While conventional edge detection algorithms such as a gradient Sobel operator or a Laplacian filter will easily identify and highlight all the boundary points, our application requires the ordered linking of these points into continuous lines. This is necessary for noise suppression, calculation of flamelet orientations, curvatures and also for the fractal dimension of the flame contours.

The technique we eventually found to be the most robust was an adaptation of a "bug" routine found in Pratt (1978). Briefly, a "bug" darts in and out of the boundary separating the bright and dark regions, turns left when it is on a bright pixel and turns right on a dark pixel (Figure 3). A number of checks are built in to rescue the "bug" from single pixel dead ends and closed loops. The algorithm always returns a series of points constituting a single-pixel thick line. The only disadvantage of the algorithm is that for curves that are not closed, the user has to specify the approximate vicinity of the starting point.

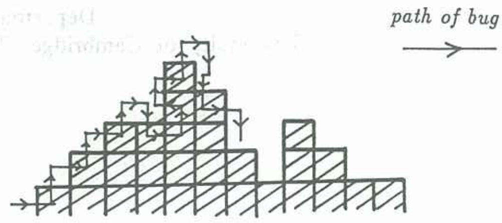

Figure 3 Path of a boundary seeking bug.

Pixel noise removal and line smoothing

The line contours extracted by the above procedure (or by any other conventional method) comprise points which fall onto a discretised grid. For the purpose of calculating the curvature and orientation of the flamelet elements, it is often necessary to sample the curve at a resolution close to one or two pixels. The noise and aliasing caused by the discretised nature of the co-ordinates makes it impossible to obtain sensible results. The problem was overcome by using a two-dimensional low-pass Fourier filter (Chew *et al* 1988). Figure 4b shows the effect of applying such a smoothing operator (computer routine taken from Press *et al* 1987) to an originally discretised curve (Figure 4a). The smoothing factor was chosen so that the features of the order of 1 pixel size are removed. The resultant co-ordinates are now generally non-integers. Curvatures and slopes can now be successfully evaluated at each point using simple polynomial and spline fits.

The same algorithm can also be applied to describe flame structure. Ziegler *et al* (1988) used progressively larger filtration factors to reduce a highly wrinkled flame contour to its fundamental frequencies. Maly *et al* (1989a, b) and Bray *et al* (1989a, b) derived mean flame positions for non-stationary engine flames using the same method and furthermore, by using a zero-level crossing argument, formulated an integral time scale of flame evolution for such flames. New and novel routines had to be developed to adequately automate the various steps and processes.

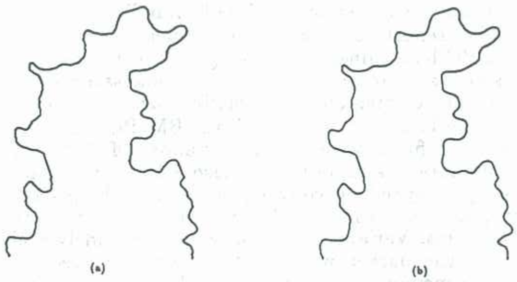

Figure 4 (a) Original flame contour (b) After Fourier smoothing.

Extraction of $\bar{c}$ contours

The quantity $\bar{c}$ represents the probability of finding combustion products. For example, the contour for $\bar{c} = 0.5$ represents the mean flame position.

To find the $\bar{c}$ contours for the Bunsen flame under discussion, we digitise a large number of the images recorded on 35*mm* film, taking care to align them according to marker points that were created during the filming. The images are then reduced to bipolar images, and then summed and averaged to obtain a picture which resembles a "time exposed" image of the flame. The contour lines corresponding to various intensities are then extracted as described in the previous section, and displayed in Figure 5a. Figure 5b shows the same contour lines but appropriately smoothed using Fourier filters. These contours are stored away and will subsequently be used extensively to find the crossing points between the mean flame contours and each individual flame. (Chew, *et al* 1989a).

The hardware limits the maximum number of images that can be averaged each time to 255. To achieve a larger ensemble, the process has to be repeated and the subsequent results averaged again.

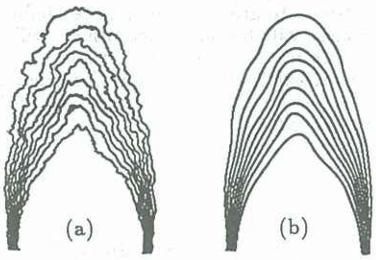

Figure 5 Lines of constant $\bar{c}$ extracted from an ensemble-averaged flame.

Fractal dimension

The most direct evaluation of fractal dimension consists of "measuring the length of the curve in question using increasingly larger measuring rules". (See for example Mandelbrot 1983). Having extracted the flame contours as an ordered series of points, it is a straightforward exercise to measure the fractal dimension. The results for an ensemble of 76 flame contours and two sets of flow conditions are shown in Figure 6. The straight lines that are fitted to the region which is deemed to exhibit fractality has slopes equal to 2-D, where D is the fractal dimension.

Other methods of measuring fractal dimensions are also available, and when the object in question does not consist of a simply connected curve, it is usually much more convenient to use a box counting routine. This essentially covers the picture with boxes of increasing size, and a plot of the number of boxes that contains the boundary against box size again yields the fractal dimension. Yet another method is to draw

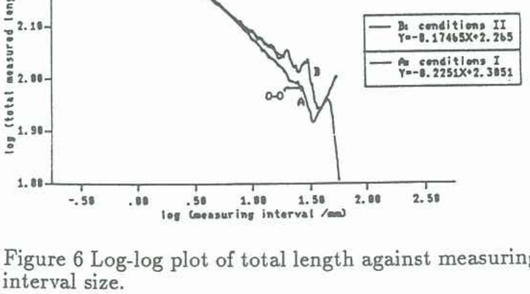

Figure 6 Log-log plot of total length against measuring interval size.

circles of increasing radius on equally spaced points on the curve (Murayama and Takeno 1988), creating a "sausage". The effective length of the "sausage" is evaluated by dividing the total area of the sausage by the radius of the circles, and a plot of effective length against the radius again yields the fractal dimension. It has been found that such box counting methods can be simulated by the use of smoothing filters in image processing. By repeating a simple 3x3 low pass filter many times, one can recreate the effect of drawing increasingly larger circles on the curve. Although in fact we are drawing increasingly large rectangles, the evaluation of the fractal dimension is not affected. However, significant savings are achieved in terms of computational time required, because the use of convolution filters is highly developed in terms of image processing hardware and algorithms.

Concentration and mixing studies

In suitably seeded or dyed flows, the relationship between concentration and the intensity of light scattered from a laser sheet can be calibrated by taking reference images, prior to or during the experiment, e.g. Shlien (1988). Similarly, non-uniformities in the laser sheet or background lighting can usually be compensated for by recording a reference frame, obtained for example by passing the laser sheet through a uniform test cell. If these simple steps are omitted, the amount of quantitative data that can be deduced from the images will be extremely limited.

Many statistical parameters of interest to concentration studies are easily obtainable from the laser sheet images. Consider the simple situation of a laser sheet-illuminated transverse cross-section of a free jet (Britter *et al* 1989). For the purpose of the argument, let us assume that the intensity of the scattered light is proportional to the concentration. In practice, this is fact be effected by programming the calibration curves into the input and output look-up tables of the image processing system. Figure 7 shows an instantaneous and an ensemble-averaged image. From the later, the mean concentration contours are easily obtained.

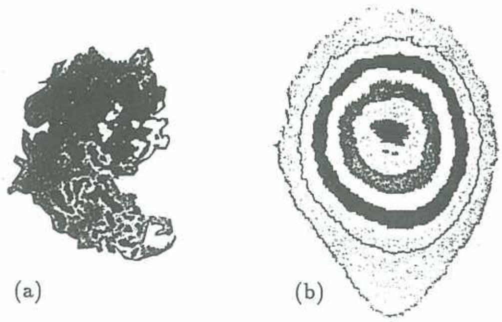

Figure 7 Instantaneous and ensemble-averaged concentration field.

A novel concept is to study the effect of measurement volume size on the concentration statistics using image processing techniques. Figure 8 shows the effect of performing low-pass filters of 5×5, 11×11 and 17×17 on an original image (a). The effect is essentially a neighbourhood averaging of pixels within the given mask size. This may correspond in real life to having measurement probes of progressively coarser resolution. Interesting results were found for the concentration fluctuations, pdf and intermittency (Britter *et al* 1989). Figure 9 shows an example, namely, the

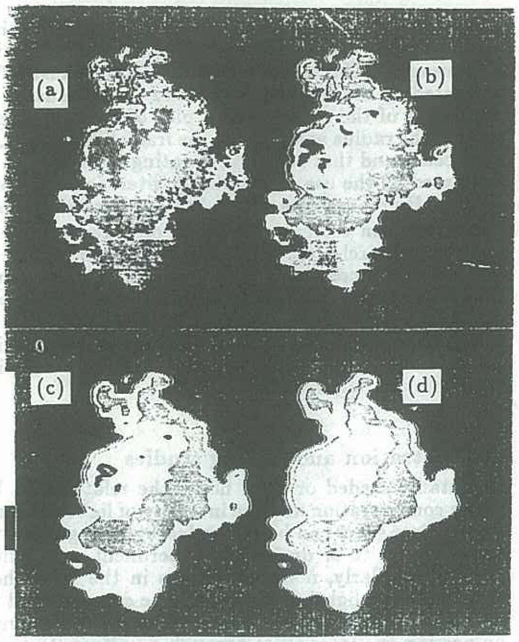

Figure 8 (a) Instantaneous concentration, (b), (c), and (d) : low-pass filtered with 5 × 5, 11 × 11 and 17 × 17 masks respectively.

effect on the concentration fluctuations at various locations in the jet as the measurement volume is increased. One advantage of using 2-D imaging is that statistics such as these, and also those for *pdf*s and intermittency, can be found for all points in the picture. For instance, a full field map of the intermittency values can be plotted out. To reduce storage requirements, a large amount of processing has to be performed on line while the tape is being played through, so that only

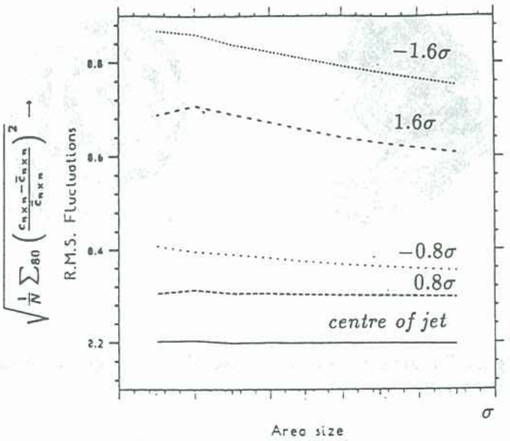

Figure 9 The effect on the concentration fluctuations at various locations in the jet.

the final result need to be stored.

Discussion

The above summary of some applications of image processing suggests that it is an extremely useful tool in flow visualisation studies of both reacting and non-reacting turbulent flows. It is slightly unfortunate that because many of the applications are different from those in conventional imaging processing work, there is little commercial software currently available to meet the needs. Apart from commissioning extensive development of customised software, the best and most flexible approach is to build up the required software in small modules for basic low-level image-processing commands. These can then be assembled in macros or modified when new a requirement arises.

Additionally, it has also been found that traditional concepts in image processing and pattern recognition can be put to good use in flow visualisation work in fluid mechanics.

Closure

One can expect that as computers and peripheral equipment become cheaper, and as quantitative flow visualisation continues to grow in importance, definitive software packages will be developed which will not only cater for basic needs like extraction and manipulation of geometrical parameters, but also for other extended applications for concentration studies and work such as particle image velocimetry.

References

Bray, K.N.C., Libby, P.A. and Moss, J.B. (1984) 20 Symp. (Int.) Combustion, p421-427, The Combustion Institute.

Bray, K.N.C., Chew, T.C. and Maly, R.R. (1989) Proc. 7th Turbulent Shear Flows Symp., p23.2.1-6, Stanford University.

Britter, R.E., Chew, T.C. and Luhar, A.K. (1989) Paper presented ar Euromech 253, Brunel University.

Chew, T.C., Britter, R.,E. and Bray, K.N.C. (1988), in "Mathematics of Deforming Surfaces", Oxford Univ. Press. *to appear.*

Chew, T.C., Britter, R.E. and Bray, K.N.C. (1989a) Combustion and Flame, **75**, p165-174.

Chew, T.C., Bray, K.N.C. and Britter, R.E. (1989b). Spatially resolved flamelet statistics for reaction rate modelling. Combustion and Flame, *to appear.*

Maly, R.R., Bray, K.N.C. and Chew, T.C. (1989a) An integral time scale of evolution for non-stationary turbulent premixed flames. Combustion Science and Technology, *to appear.*

Maly, R.R., Chew, T.C., Bray, K.N.C., Pfister, W., Eberspach, G. and Geiger, K. (1989b) Paper presented at "Motorische Verbrennung, Essen, West Germany.

Mandelbrot, B.B. (1983) The Fractal Geometry of Nature. Freeman, New York.

Press, W.H., Flannery, B.P., Teukolsky, S.A. and Vetterling, W.T. p495-497, *Numerical Recipes*, Cambridge University Press, 1987.

Pratt, W..K. (1978) Digital Image Processing, Wiley Interscience.

Shlien, D.J. (1988) Expts. Fluids **6**,p541-546.

Ziegler, G. (1988) SAE paper 881636.